Transition State Structures and Intermediates Modeling Carboxylation Reactions Catalyzed by Rubisco. A Quantum Chemical Study of the Role of Magnesium and Its Coordination Sphere

Mónica Oliva, Vicent S. Safont,* and Juan Andrés

Departament de Ciències Experimentals, Universitat Jaume I, Box 224, 12080 Castelló, Spain

O. Tapia

Department of Physical Chemistry, Uppsala University, Box 532, S-75121 Uppsala, Sweden

Received: April 10, 2001; In Final Form: June 14, 2001

The reactive sequences mimicking the carboxylation chemistry catalyzed by Rubisco are characterized at HF/3-21G and HF/6-31G** calculation levels. Hydroxypropanone, $C^1H_3-C^2O-C^3H_2OH$, represents the substrate D-ribulose-1,5-bisphosphate, while the enzyme active site is modeled with residues found at the coordination sphere of magnesium: a carbamylated ammonia (Lys 201), two formiate (Asp 202 and Glu 204), and one water molecule. Theoretical characterization of saddle points of index one, transition state (T-S) structures, starts with an intramolecular enolization process previously reported, yielding an enediol intermediate (carbonyl oxygen at C^2 is transformed into alcohol, C^2-OH). The CO_2 addition, with a concomitant hydrogen transfer from the C^3-OH to carbon dioxide constitutes the second step, with formation of a carboxy-ketone (carboxy-aldehyde in our model) intermediate, $C^1H_3-C^2OH(COOH)-C^3HO$. Adding a water molecule at C^3 is the third step, followed by the C^2-C^3 bond break. This process is coupled with another intramolecular hydrogen transfer, yielding in the real substrate 3-phospho-D-glycerate and an intermediate. A final step involving this intermediate is associated with the C^2 inversion with formation of another molecule of 3-phospho-D-glycerate. A detailed comparison of T-Ss with and without inclusion of the residues forming the magnesium coordination sphere is presented. Except for the already reported enolization T-S and also for one of the C^2-C^3 bond rupture T-Ss, the key geometric elements and the amplitudes of the transition vectors are fairly invariant to the presence of the magnesium coordination sphere. The reported transition structures are joined in order by appropriate precursor and successor complexes reflecting the real chemistry. The present model can hence be related to a sequential ordered kinetics. Most experimental aspects of the reaction pathways catalyzed by this key enzyme find explanation within the molecular mechanism obtained from the present theoretical results.

Introduction

In a recent paper,[1] the oxygenation chemistry, as it appears catalyzed by Rubisco, was theoretically characterized with transition structures (T-Ss) describing enolization, oxygen fixation, hydration, and concerted O−O and C^2-C^3 bond breaking. Hydroxypropanone, $C^1H_3-C^2O-C^3H_2OH$, was used to model the chemically active groups in the substrate RuBP (D-ribulose-1,5-bisphosphate). This model was embedded in the Mg coordination shell including a model carbamylated lysine.

As it is well-known, RuBP can react with carbon dioxide leading to the atmospheric carbon dioxide fixation at its C^2 center. The mechanism involves a complex chemistry starting from the enolization step and followed by carbon dioxide fixation, hydration of C^3, bond breaking of C^2-C^3, and configuration inversion at the C^2 center. Two molecules of 3-phospho-D-glycerate (PGA) are released from the active site. In previous works we have identified a set of saddle points of index one using hydroxypropanone as the initial model substrate that corresponds to the steps of this mechanism.[2,3] Here, the effects of the magnesium coordination shell onto the T-Ss in the carboxylation path are studied.

We have shown that all the carboxylation and the oxygenation chemistry can be described with a minimal 3-carbon (3C) molecular model [2,4] and have tested a 5-carbon (5C) molecular model with identical results.[5] This situation allows us to use the 3C model. Recently, Ornstein and co-workers [6] have used 2C and 4C molecular models to study several alternative pathways for carboxylation and hydration, exploring the effect of water solvent, and analyzing the intramolecular hydrogen bonding as stabilizing factor. At variance with our work, this study explores a nonenzymatic RuBP carboxylation chemistry. In the enzymatic carboxylation chemistry studied by us, for each step, a well-defined T-S describes the conversion with the help of related precursor and successor complexes. The successor complex of a given step appears as a partner to form the precursor complex of a following step. This finding leads to the intramolecular mechanistic description of Figure 1. At variance with early mechanistic proposals based upon general acid/base catalysis by selected residues of the enzyme, the picture presented here corresponds to a set of intramolecular hydrogen exchange processes in a molecular model sustaining all the chemistry. Concerted bond snipping and knitting reminding of reactive radicals in a cage[7] is suggested by the electronic structure of the T-Ss. This alternative mechanism does not require enzyme residues acting as proton donors or acceptors to accomplish the chemistry.

10.1021/jp0113533 CCC: $20.00
Published on Web 09/13/2001

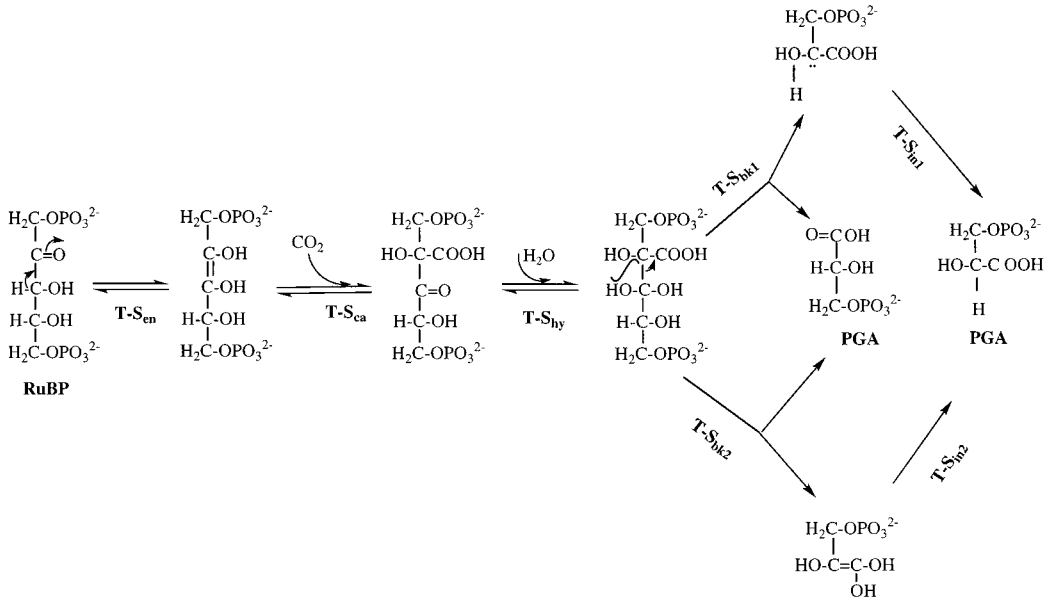

Figure 1. Schematic representation of a reaction pathway for the carboxylation of RuBP catalyzed by Rubisco. **T-S$_{en}$**, **T-S$_{ca}$**, **T-S$_{hy}$**, **T-S$_{bk}$**, and **T-S$_{in}$** refer to the T-Ss for the enolization, CO_2 addition (or carboxylation), hydration, C^2-C^3 bond breaking, and C^2 configuration inversion steps, respectively. For the T-S$_{bk}$ and T-S$_{in}$, two alternatives (1 and 2) have been studied. When the magnesium coordination sphere is included, a final -S is added to the T-S notation.

The studies of T-Ss in a vacuum raise skepticism because it is believed that the enzyme will somehow change the whole picture. This may be so even for the present case. The point with our approach is to try disentangling, as much as it is possible, the effects of the protein onto the electronic mechanism. To fulfill this goal, we have checked that all T-Ss present invariance to model size (3C or 5C), and level of wave function representation of electronic theory.[2−5,8−10] The problem now is the evaluation of the role played by the enzyme: Is there any reason to believe that, once the complexities of the active site are introduced in the calculations, one would get the same mechanistic picture in terms of similar transition structures? The answer to this question has general implications to molecular modeling. As discussed below, there are many more aspects to the role of the protein that can be discussed from the standpoint of our models in absence of the enzyme. However, for the present system the more serious criticism comes from the fact that magnesium is essential for catalysis. Moreover, to activate the protein, a lysine residue should react with a carbon dioxide molecule (different from the one entering in the carboxylation step) leading to a carbamate. This modified residue together with an aspartate and a glutamate provide the coordination shell for magnesium. What is the effect of magnesium on the saddle point structures characterizing the T-Ss of the minimal molecular model? This problem is addressed here in what concerns the carboxylation pathway.

In the preceding oxygenation papers,[1,11] the geometry of the enolization T-S was found to be modified due to the Mg coordination sphere presence, while the geometry of the rest of T-Ss was unchanged. The resulting enolization T-Ss may act as a precursor fragment in the formation of the oxygenation saddle point of index one at the coordination sphere. The structural effect was identified as hydrogen bonding to the enolization-T-S originated from the carbamate oxygen not involved in magnesium bonding. The proximity of the triplet state in the twisted conformation allowed for a rationalization of the spin intersystem crossing. We observe that the same T-S for enolization is the fragment to enter in the precursor complex of carboxylation. It is therefore important to accurately characterize all carboxylation saddle point structures into the magnesium coordination sphere and compare the results with the T-Ss in its absence.

The model and computing methods are the same as those reported earlier,[1] except that B3LYP/6-31G** is not used: it was found that it gave no noticeable differences for the T-Ss (as for geometry and transition vector is concerned) with a much larger computation cost. All calculations were carried out using the GAUSSIAN 94[12] and GAUSSIAN 98[13] programs. Supplementary vibration analysis is made with the Gaussview[14] package. The results are presented together with the examination of the mechanistic determinants that have been derived from different experiments.

T-Ss and Mechanistic Determinants. The transition structures implied in Figure 1 are depicted now in Figure 2 for the Mg-coordination model. The carboxylation saddle point, **T-S$_{ca}$−S** (**S** stands for sphere), and consecutively the hydration T-S (**T-S$_{hy}$−S**) are found. By using the 3C model without magnesium, two T-Ss were also obtained (**T-S$_{ca}$** and **T-S$_{hy}$**). From this point onward, two alternative pathways,[15] including C^2-C^3 bond breaking and C^2 configuration inversion, are characterized.

The saddle point associated with the C^2-C^3 bond breaking, previously obtained with the 3C (**T-S$_{bk1}$**) and 5C models,[2,3,5,15,16] has not been recovered yet in the magnesium coordination sphere.[16] The geometry optimization yields a too strong $Mg-O^3$ interaction that seems to explain this result. This hypothesis was tested by actually getting a saddle point (**T-S$_{bk1}$−S**) by avoiding full geometry optimization (at HF/3-21G level) between the coordination sphere and the reactive motif. The T-S corresponding to C^2 configuration inversion (**T-S$_{in1}$** and **T-S$_{in1}$−S**) was characterized.

For the other pathway, all four T-Ss are properly determined, either with the 3C model (**T-S$_{bk2}$** and **T-S$_{in2}$**) or by using the enlarged model (**T-S$_{bk2}$−S** and **T-S$_{in2}$−S**). A comparison between the two pathways is reported below.

Several details concerning the mechanism of the reactions catalyzed by Rubisco enzyme, for carboxylation pathway, have been established from experimental works. The ensemble of

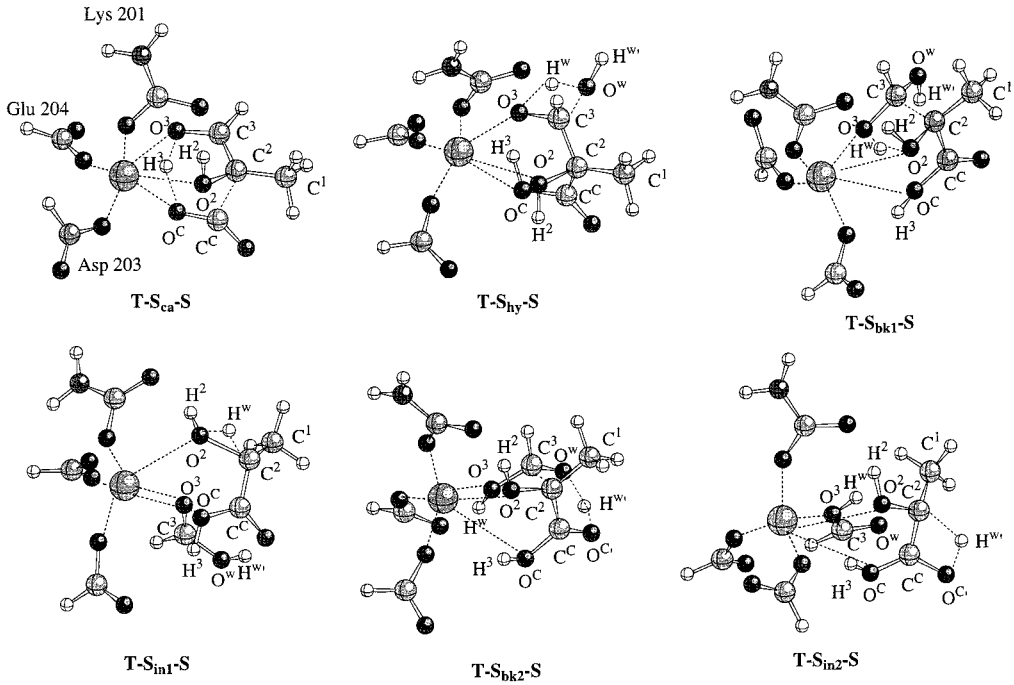

Figure 2. T-Ss obtained for the model including the Mg coordination sphere, at HF/3-21G level. Dashed lines represent bonds that are being broken/formed or coordination interactions between the Mg and its ligands. Atom numberings are indicated.

the facts that are relevant to discuss our results is summarized below; we use the theoretical results to establish a relationship to the experimental facts.

1. Rubisco is capable to catalyze a whole set of reactions one after another.[17] For this to be possible, it seems reasonable to expect that when a catalytic cycle ends, Rubisco's active site be left in the same state as before the beginning of it. This is obvious, but some studies have failed to consistently explain the involvement of acid/base chemistry in the reaction mechanism of Rubisco. The intramolecular nature of the mechanisms reported here avoids these difficulties in a refined way. Moreover, the concatenated nature of the different transition structures is in full agreement with the work of Miziorko and Lorimer.[17]

2. The gaseous substrates come from the active site's exterior.[18] This idea reflects the fact that the gaseous substrates do not form Michaelis complexes with the protein. The theoretical results point to the necessity of the enolization transition structure, previously reported by us.[1] Either carbon dioxide or molecular oxygen must form a precursor complex with the *successor* of the enolization T-S.

3. The substrate bound to the activated Rubisco has a definite orientation.[18] Today, with the X-ray studies this conclusion is obvious. But, for our molecular models where most of the protein is not present, the constraint makes sense. The theoretical stationary geometry structures show definite orientations of the gaseous substrates and the model RuBP in the coordination sphere of magnesium. Overlay of the theoretical geometry with X-ray data show that the relative orientation of the reactants is fully compatible with the space available at the active site. In this sense, the electronic properties of the simple model elicit some important results derived from experiments.

4. Rubisco catalyzes the appearance of solvent tritium at C^3 of RuBP.[19] This was interpreted as a proof of the enediol (or enediolate) intermediate, and as evidence that the C^3 bound hydrogen has to move to a place where exchange with solvent hydrogen is possible. The intramolecular enolization transition structure[1] (not shown) has the properties required to explain those results. The alcohol group formed at C^2 can exchange hydrogen with the solvent once the enediol is formed. Retro-enolization[8] to RuBP would put this hydrogen (incorporated from solvent) to C^3.

5. There exists a six-carbon intermediate in the carboxylation process.[17,20,21] This intermediate has been characterized after washing the active site. Because of the procedure, it is not clear if such intermediate is just the result of the carboxylation of enediol intermediate,[22] or the result of the carboxylation and simultaneous hydration of such intermediate.[23]

The carboxylation transition structure **T-S$_{ca}$**, in the absence of magnesium, has been already determined.[2,5] In Figure 3, the same T-S is reported in the coordination sphere of magnesium (**T-S$_{ca}$−S**) and compared with the simple model. In Table 1 the geometric parameters are listed. The invariance of the transition vector (TV) and geometric parameters is a striking result, and we have shown this invariance to be true even if the enzyme itself is taken into account.[9] Just a small difference can be sensed in Figure 3 and Table 1: the H^3 passage from O^3 to O^C is more advanced in the small model (mainly at HF/6-31G** level).

The fluctuations that the corresponding TVs describe correspond with the C^2-C^C bond forming process, accompanied by the H^3 migration from O^3 to O^C. The T-S involves six atoms, disposed in a rough hexagonal conformation (see Figure 3 and Scheme 1). Two putative π bonds (C^2-C^3 and O^C-C^C) and a putative σ bond (O^3-H^3) are broken, while two σ (C^C-C^2 and H^3-O^C) and one π (O^3-C^3) bonds are knitted. A strong hydrogen bond is detected between the Lys 201 oxygen atom (O^L) and the H^2 atom (see Table 1).

The successor complex would correspond to the six-carbon intermediate. The mechanism requires the hydroxyl group at C^3 whose hydrogen is transferred to the activated carbon dioxide. The dihedral angle $O^2-C^2-C^3-O^3$ corresponds to a fragment in cis out-*of*-plane conformation. The precursor complex has no enediol structure. It is rather a twisted diol. This arrangement helps activating the C^2 center toward carbon dioxide attack, and activation of C^3. This latter effect is coupled to the propensity

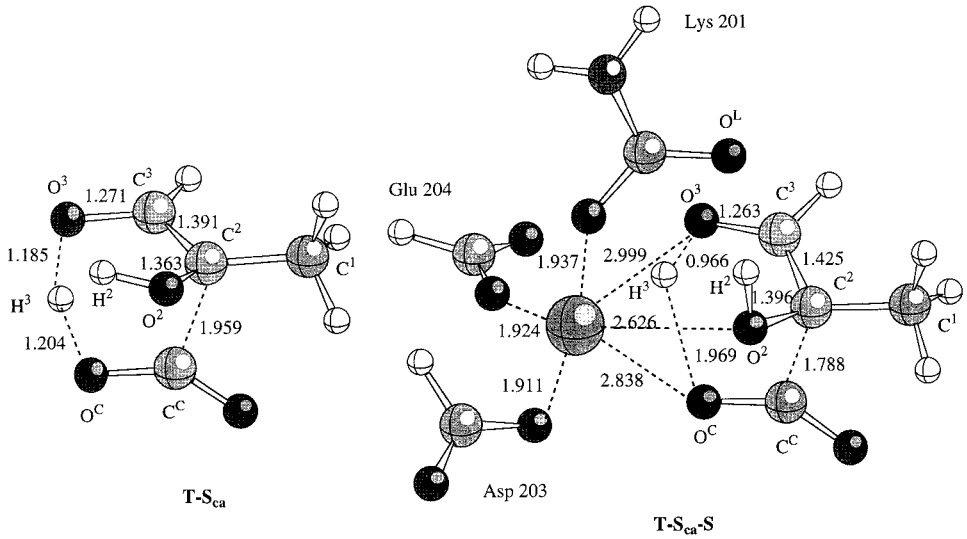

Figure 3. T-Ss for the CO_2 addition step: **T-S$_{ca}$** (3C model) and **T-S$_{ca}$−S** (model including the Mg coordination sphere). Some distances in angstroms are indicated, calculated at HF/6-31G** level. Dashed lines represent bonds that are being broken/formed or coordination interactions between the Mg and its ligands. Atom numberings are indicated.

SCHEME 1: Homolytic Pericyclic Mechanism for the CO_2 Addition T-S

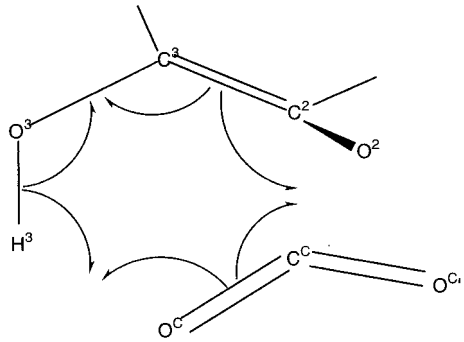

of the hydroxyl group in C^3 to become a carbonyl group when the hydrogen is shifted toward the carbon dioxide. The T-S elicits all these properties in its geometry and reactivity indexes. As mentioned above, the carboxylated successor complex is the analogue to the six-carbon atom intermediate. In view of the space available at the active site, the molecular structure would be molded with geometry similar to that of the T-S.

6. H_2O addition occurs in the carboxylation process. However, it is not well established if the water attack occurs from the same side of CO_2 attack or from the opposite, neither is it clear whether the additions occur consecutively[21,22,24] or simultaneously.[23,25]

The direction into which a water molecule may attack C^3 is actually determined by the stereochemistry of both RuBP enolization and CO_2 addition at the coordination shell of the metal. If we divide this shell in two hemispheres, the residues Asp 203, Glu 204 and carbamylated Lys 201 occupy the first hemisphere. The second hemisphere contains the substrate's oxygen atoms (see Figure 3). Their positions are in fairly well agreement with the corresponding atoms in 2-carboxy-D-arabinitol 1,5-bisphosphate (CABP) inhibitor complex determined by Inger Andersson.[26] The nonplanar substrate moiety $O^2-C^2-C^3-O^3$ occupies two positions in the second hemisphere. The third slot in the coordination shell is occupied by water before the gaseous substrate enters.

After the gas substrate binding, an oxygen atom from carbon dioxide, displaces the water molecule thereby completing the coordination shell again. Either this displaced water molecule, or another coming from solvent and trapped in the enzyme, can be used in the hydration step. Then, within the present model, the water molecule can only enter from the same side as carbon dioxide.

The hydration transition structure in the coordination shell has a similar structure to the one found in the minimal molecular model. In Figure 4 and Table 1 the T-Ss (**T-S$_{hy}$** and **T-S$_{hy}$−S**) are presented.

From the data in Table 1, it is apparent the invariant character of these T-Ss with respect to the calculation level as well as with respect to the molecular model size. The fluctuations described by the TV correspond to the water addition to the carbonyl group at C^3: the oxygen from water molecule (O^w) binds to C^3, while one of the water hydrogen (H^w) binds to O^3. The T-S has four centers ring character, and a gemdiol is formed along the intrinsic reaction coordinate (IRC)[27] to products (not shown).

Mechanistically, hydration must take place after formation of the carboxylation structure. For in this case, the initial alcohol group (in RuBP) at C^3 is transformed into a carbonyl double bond species. Water acts onto the carbonyl group leading, as explained, to gemdiol at C^3. This result agrees with indirect experimental evidence. The successor complex (gemdiol) was used in the simple model to describe one of the most remarkable properties of the present mechanism, the C−C bond breaking. This was achieved via a hydrogen transfer from one of the OH groups toward either the oxygen in the hydroxyl group at C^2 or, in the alternative path discussed in the present work, toward the carboxylated group derived from the carbon dioxide fixation.

7. The only product of the carboxylation process is PGA.[17,20,21] This implies a C^2-C^3 bond breaking and configuration inversion at C^2 center during the carboxylation process. The successor complex of the C^2-C^3 bond snipping was used in previous works to study the inversion by a 1,2-hydrogen shift from O^2 toward C^2.[2,3,5,15] For the 3C model, we have found the **T-S$_{bk1}$** associated with the C^2-C^3 bond-breaking step as well as with the H^w transfer between O^3 and O^2 (Figure 5). The same stationary point within the coordination shell was not found as true T-S. Instead, a saddle point (**T-S$_{bk1}$−S**) was located as the result of a weak optimization for the molecular motif, see above.

TABLE 1: Geometric Parameters (Distances in angstroms, Dihedral Angles in Degrees) Calculated for the Indicated T-Ss, at the Calculation Level Shown: A Comparison of the Effect of the Mg Coordination Sphere upon the Geometries of the T-Ss Can Hence Be Done

	HF/3-21G		HF/6-31G**	
	$T\text{-}S_{ca}$	$T\text{-}S_{ca}\text{-}S$	$T\text{-}S_{ca}$	$T\text{-}S_{ca}\text{-}S$
$C^2\text{-}C^3$	1.387	1.389	1.391	1.425
$C^3\text{-}O^3$	1.296	1.293	1.271	1.263
$O^3\text{-}H^3$	1.221	1.123	1.185	0.966
$H^3\text{-}O^C$	1.214	1.351	1.204	1.969
$O^C\text{-}C^C$	1.250	1.250	1.233	1.220
$C^C\text{-}C^2$	1.960	1.892	1.959	1.788
$O^L\text{-}H^2$		1.523		1.739
$O^2\text{-}C^2\text{-}C^3\text{-}O^3$	−27.79	−38.8	−25.41	−44.53

	HF/3-21G		HF/6-31G**	
	$T\text{-}S_{hy}$	$T\text{-}S_{hy}\text{-}S$	$T\text{-}S_{hy}$	$T\text{-}S_{hy}\text{-}S$
$C^2\text{-}C^3$	1.504	1.518	1.519	1.527
$C^3\text{-}O^w$	1.589	1.570	1.554	1.533
$O^w\text{-}H^w$	1.128	1.121	1.121	1.114
$H^w\text{-}O^3$	1.399	1.417	1.342	1.354
$O^3\text{-}C^3$	1.371	1.408	1.329	1.353
$O^3\text{-}H^3$	1.428	1.451	1.457	1.452
$H^3\text{-}O^C$	1.024	1.005	0.977	0.969
$O^L\text{-}H^2$		4.532		4.788
$O^2\text{-}C^2\text{-}C^3\text{-}O^3$	−69.01	−71.59	−67.01	−69.7

	HF/3-21G		HF/6-31G**
	$T\text{-}S_{bk1}$	$T\text{-}S_{bk1}\text{-}S$	$T\text{-}S_{bk1}$
$C^2\text{-}C^3$	2.228	1.628	2.299
$C^3\text{-}O^3$	1.265	1.397	1.238
$O^3\text{-}H^w$	1.947	1.452	1.659
$H^w\text{-}O^2$	0.992	1.348	0.976
$O^2\text{-}C^2$	1.565	1.517	1.557
$O^L\text{-}H^2$		1.504	
$O^2\text{-}C^2\text{-}C^3\text{-}O^3$	−43.82	−48.3	−34.89

	HF/3-21G		HF/6-31G**	
	$T\text{-}S_{in1}$	$T\text{-}S_{in1}\text{-}S$	$T\text{-}S_{in1}$	$T\text{-}S_{in1}\text{-}S$
$C^2\text{-}O^2$	1.616	1.614	1.598	1.600
$O^2\text{-}H^w$	1.129	1.123	1.097	1.096
$H^w\text{-}C^2$	1.357	1.365	1.319	1.323
$O^2\text{-}H2$	0.978	0.997	0.951	0.961
$C^2\text{-}C^C$	1.425	1.432	1.440	1.453
$O^L\text{-}H^2$	−	2.142	−	2.381

	HF/3-21G		HF/6-31G**	
	$T\text{-}S_{bk2}$	$T\text{-}S_{bk2}\text{-}S$	$T\text{-}S_{bk2}$	$T\text{-}S_{bk2}\text{-}S$
$C^2\text{-}C^3$	2.057	2.087	1.939	1.995
$C^3\text{-}O^w$	1.285	1.282	1.264	1.257
$O^w\text{-}H^{w'}$	1.296	1.252	1.406	1.348
$H^{w'}\text{-}O^{C'}$	1.159	1.153	1.062	1.066
$O^{C'}\text{-}C^C$	1.294	1.294	1.276	1.278
$C^C\text{-}C^2$	1.375	1.382	1.392	1.392
$O^L\text{-}H^2$		1.658		1.833
$O^2\text{-}C^2\text{-}C^3\text{-}O^3$	−45.36	−39.09	−48.05	−39.92

	HF/3-21G		HF/6-31G**	
	$T\text{-}S_{in2}$	$T\text{-}S_{in2}\text{-}S$	$T\text{-}S_{in2}$	$T\text{-}S_{in2}\text{-}S$
$C^2\text{-}C^C$	1.454	1.417	1.447	1.425
$C^C\text{-}O^{C'}$	1.277	1.290	1.251	1.260
$O^{C'}\text{-}H^{w'}$	1.251	1.274	1.213	1.231
$H^{w'}\text{-}C^2$	1.554	1.570	1.525	1.533
$O^L\text{-}H^2$		1.617		1.844

This saddle point is also presented in Figure 5. Selected geometric parameters for the different T-Ss are listed in Table 1.

The effect of the coordination shell on this T-S is apparent. In fact, it could not be located when the coordination shell enters into the molecular model. There is formation of a relatively strong $Mg\text{-}O^3$ bond as elicited by a previously reported analysis[16] of the Electron Localization Function. As a result, the $C^2\text{-}C^3$ distance in the $\mathbf{T\text{-}S_{bk1}\text{-}S}$ structure is shorter than that in $\mathbf{T\text{-}S_{bk1}}$, and there is no bond breaking process along the IRC pathway. The H^w transfer and the $C^2\text{-}C^3$ bond breaking processes are uncoupled now: the TV of the reported saddle point ($\mathbf{T\text{-}S_{bk1}\text{-}S}$) is associated with the hydrogen transfer only. Again, a strong hydrogen bond between O^L and H^2 can be sensed in this structure.

To decide whether the explained uncoupling effect is just a consequence of the models and methods used, or if it reflects a real situation, and consequently this mechanistic pathway is a nonexit path, it is necessary to include the protein in a more realistic manner. This work is being planned at a QM/MM level, and it corresponds to the final step in the study of the molecular mechanism.

The corresponding configuration inversion at C^2 center can still be studied. The transition structures ($\mathbf{T\text{-}S_{in1}}$ and $\mathbf{T\text{-}S_{in1}\text{-}S}$) are reported in Figure 6 and Table 1. The 1,2-H transfer can be accomplished without any steric hindrance from the coordination shell. The invariance of these stationary points with respect to the calculation level and model size is apparent. It is interesting to note the presence of a strong hydrogen bond between O^L and H^2 again. This interaction can fix this hydrogen and make H^w the only hydrogen capable to transfer from O^2 to C^2; in this manner the configuration inversion takes place and the only product has a D-configuration around the C^2 center. Once more, Lys 201 residue appears to play a fundamental role in our model calculations. This is much rewarding since the whole set of results show remarkable consistency.

An alternative pathway for these two steps was characterized and found to be possible for our models.[15] In fact, within this alternative pathway, both the $C^2\text{-}C^3$ bond breaking T-S ($\mathbf{T\text{-}S_{bk2}}$ and $\mathbf{T\text{-}S_{bk2}\text{-}S}$) and the configuration inversion at C^2 center T-S ($\mathbf{T\text{-}S_{in2}}$ and $\mathbf{T\text{-}S_{in2}\text{-}S}$) can be found without problems as true T-Ss, with the two molecular models used. In Figures 7 and 8, and in Table 1, the transition structures are presented.

The $C^2\text{-}C^3$ bond breaking is described also as associated with a hydrogen transfer, this time between O^w and $O^{C'}$, leading to a gem-enetriol. Very small differences on the geometric parameter values can be found in Table 1 depending on the calculation level. The fluctuation pattern described by the TV is invariant, and corresponds to a collective motion of six centers (see Figure 7): a π bond is broken ($C^C\text{-}O^{C'}$) while two are formed ($C^3\text{-}O^w$ and $C^C\text{-}C^2$), and two σ bonds break ($C^2\text{-}C^3$ and $O^w\text{-}H^{w'}$) while one forms ($O^{C'}\text{-}H^{w'}$).

The configuration inversion at C^2 process is now described as a four center ring, with a hydrogen migration from $O^{C'}$ to C^2, accomplishing the inversion at C^2. However, it is possible to imagine an equivalent structure, with migration of $H^{w'}$ from $O^{C'}$ to C^2 but without configuration inversion. To further explain the selectivity observed for product formation in this pathway, one has to look for interactions with protein residues that are not included in the present model, and to calculate significant energies to make a comparison. The QM/MM calculations that are being conducted should be giving additional clues to explain this issue.

8. The fate of some hydrogen atoms has been experimentally established during the carboxylation.[19,28−30] Isotopic label of the C^3 hydrogen on RuBP does not appear in the products. Either this hydrogen atom ends up on a group capable of exchanging protons with the solvent or directly out of the products structures.[19,29,30] Solvent protons appear bounded to C^2.[19,28,29]

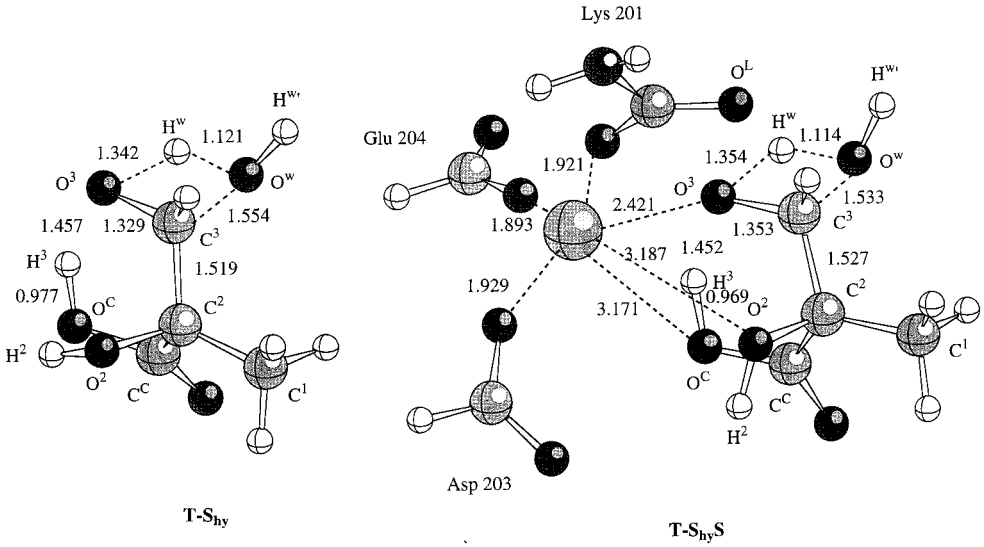

Figure 4. T-Ss for the hydration step: **T-S$_{hy}$** (3C model) and **T-S$_{hy}$−S** (model including the Mg coordination sphere). Some distances in angstroms are indicated, calculated at HF/6-31G** level. Atom numberings are indicated.

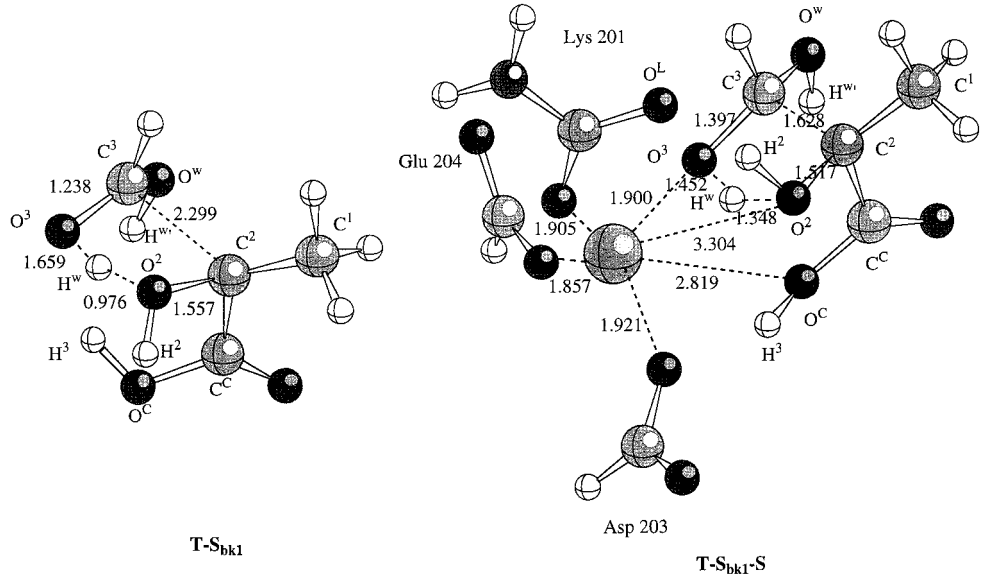

Figure 5. T-S for the C^2-C^3 bond breaking step: **T-S$_{bk1}$** (3C model). Some distances in angstroms are indicated, calculated at HF/6-31G** level. For the model including the Mg coordination sphere a true T-S was not found. Instead, a saddle point obtained from a weak geometry optimization at HF/3-21G level for the molecular motif (**T-S$_{bk1}$−S**) is shown. Some distances in angstroms are also indicated. Atom numberings are indicated.

The T-Ss and intermediates reported here are fully compatible with these experimental results. The C^3 hydrogen of RuBP (here named as H^2 because in the enolization step it was moved from C^3 to O^2) ends up in the OH group of the central carbon of one product molecule (see Figure 6 or Figure 8). This is a group capable of exchanging protons with the solvent, as required. On the other side, the H attached to C^2 at the end of the catalytic cycle comes from the water molecule entering in the hydration step, as required also (see Figure 2, Figure 6 or Figure 8).

Bond Breaking-forming Mechanisms from the TSs

To understand the electronic changes associated with the carboxylation and oxygenation chemistry, it is useful to employ some concepts developed for the description of carbon−carbon formation between reactive radicals in a cage by Turro et al.[7] The concept appears to be useful in connection with the description of the T-Ss presented so far.

The radical character of these reactions can be induced by the existence of a triplet state related to the enediol structure. The planar conformer, cis or trans, has a singlet spin electronic structure. The triplet is the lowest state for the conformer having a dihedral angle of 90°. The twisted conformation of $O^2-C^2-C^3-O^3$ may be seen as a way to mix the triplet to the singlet spin wave functions. If we look at the precursor complex for carboxylation and compare it to the successor (not shown), we can see an extensive change of hybridization state for the centers entering the reaction. One has to break bonds and concomitantly form other bonds to achieve the chemistry.

Let us consider the carboxylation T-S. In Scheme 1 the homolytic pericyclic mechanism is displayed. To transform carbon dioxide into a carboxylic acid group, the sp carbon hybridization must be changed into a sp^2. This can be obtained by breaking an O=C π bond and flipping the oxygen orbital with a dangling bond. The carbon atom should show a sp^2 dangling bond. The C^2 center must accordingly be activated. This is achieved by the torsion of $O^2-C^2-C^3-O^3$ around the C^2-C^3 bond. The breaking of the dienol is required to perform a bond (spin) pairing with the dangling bond in carbon dioxide.

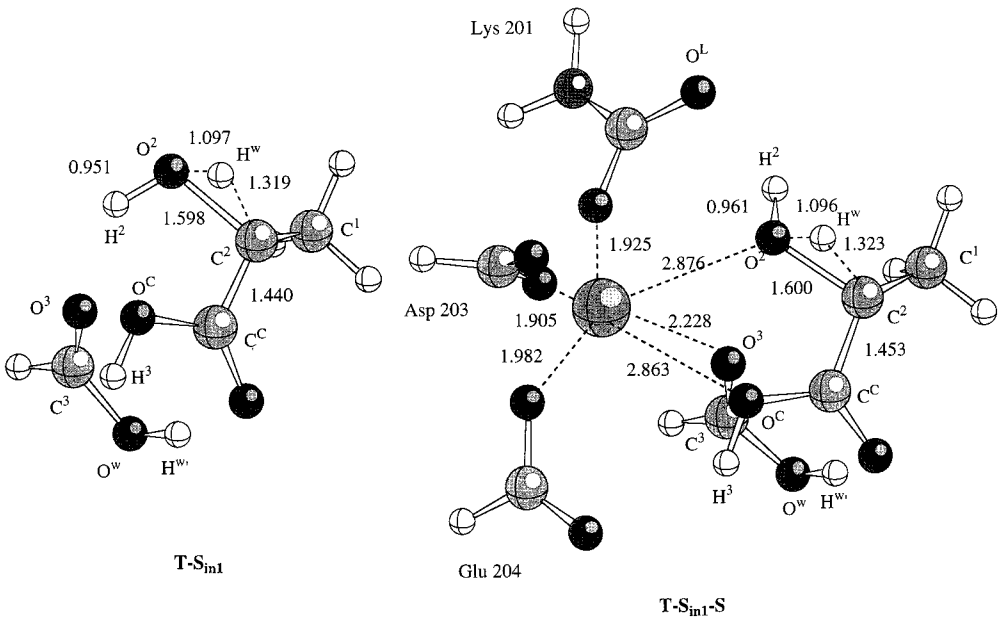

Figure 6. T-Ss for the C^2 configuration inversion step: **T-S$_{in1}$** (3C model) and **T-S$_{in1}$−S** (model including the Mg coordination sphere). Some distances in angstroms are indicated, calculated at HF/6-31G** level. Atom numberings are indicated.

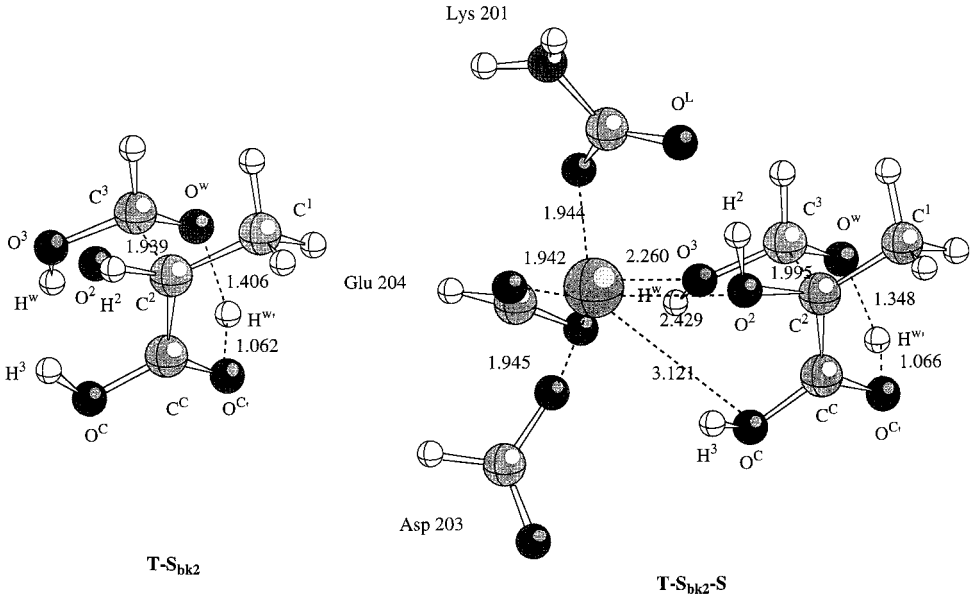

Figure 7. T-S for the C^2-C^3 bond breaking step: **T-S$_{bk2}$** (3C model) and **T-S$_{bk2}$−S** (model including the Mg coordination sphere). Some distances in angstroms are indicated, calculated at HF/6-31G** level. Atom numberings are indicated.

The hydrogen to be transferred from the O^3-H^3 toward the CO_2 (O−H bond breaking) would accomplish two results: (i) activate the $C^C=O^C$ bond in CO_2 and (ii) produce a dangling orbital at O^3. The $C^2=C^3$ breaking releases a dangling orbital at C^3 that will form the π bond $C^3=O^3$ in the successor complex. The required spin unpairing-pairing accomplishing the electronic reshuffling must be helped by the triplet electronic state.

The processes described above correspond to our homolytic bond breaking/forming mechanism discussed in previous publications.[1,11,16]

To understand the steps following CO_2 fixation, it is useful to examine the electronic structure related to the gemdiol and the carbon−carbon bond rupture. The fragment $O^2-C^2-C^3-O^3$ has a geometry where the C^2-C^3 double bond is twisted and therefore it counts as a single bond. C^3 has four valence bonds. If one transforms a single HO^3-C^3 bond into a carbonyl group $O^3=C^3$ bond, one may expect the C^2-C^3 bond to break under certain conditions. If the hydrogen is transferred to the hydroxyl group at C^2, it creates the conditions necessary for the formation of an *aci*-acid-like group. An alternative is the transfer to the carbonyl oxygen atom of carboxylic group, forming in this case a twisted enetriol intermediate, which would prompt for hydrogen rearrangement to PGA. As we have pointed out, all these electronic rearrangements should be described as homolytic bond breaking and forming thereby relating this type of process to spin stereochemistry in carbon−carbon chemistry in radicals.[7] The enzyme active site provides the cage trapping the intermediate radical structures and allowing for the advance of the reaction.

The results discussed above suggest that carbon dioxide must bind to the activated substrate. This is the successor complex of the enolization transition structure. Therefore, no standard Michaelis complex can be expected. This is in agreement with the kinetic mechanism of Rubisco, which is described as a

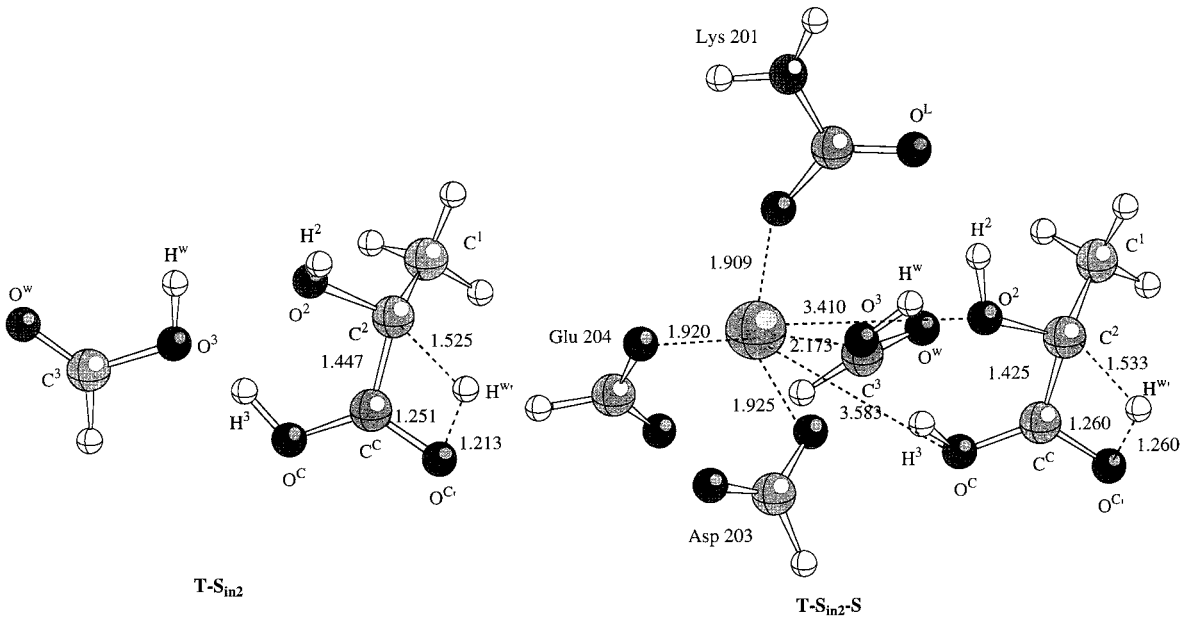

Figure 8. T-Ss for the C^2 configuration inversion step: **T-S$_{in2}$** (3C model) and **T-S$_{in2}$−S** (model including the Mg coordination sphere). Some distances in angstroms are indicated, calculated at HF/6-31G** level. Atom numberings are indicated.

modified Theorell−Chance mechanism; the process is sequentially ordered. RuBP binds first forming a Michaelis complex.[31,32] Thereafter, carbon dioxide reacts with second-order kinetics to the activated intermediate. The agreement of the theoretical results with the kinetic mechanism is quite satisfactory.

Final Remarks

The intramolecular nature of the present mechanism has two important catalytic aspects. First, a role of the transferred hydrogen atom appears to be a way to induce orbital steering. Second, the intramolecular mechanism ensures that at the end of the catalytic cycle the coordination shell and the protonation state of side chains are left as they were at the beginning. Once the loop 6 (spinach) is open,[21] the products may diffuse toward the solution and the active site is left in the same state as it was and a new catalytic cycle can take place.

All the argument is based upon shape complementarity of stationary geometries related to precursor and successor complexes. If one want to examine the energetic aspects of the enzyme catalyzed reaction, the phosphate groups in the substrate and the protein atoms must be included. Still, it is of interest to look at energy issues with the present model. A first rough approximation can be obtained from the Born−Oppenheimer free energy values for the calculated T-Ss, relative to **T-S$_{ca}$**, or **T-S$_{ca}$−S**, plus a water molecule. These free energy values are presented in Table 2 for the two models and theoretical levels used. As one can expect, the results are dependent on the nature of the basis set. The main trends are conserved.

At the HF/3-21G level, for the 3C model, **T-S$_{hy}$** stands 3.2 kcal/mol above the reference and then the energy raises to **T-S$_{bk1}$** (18,6 kcal/mol) and to **T-S$_{in1}$** (24,4 kcal/mol). The bond-breaking step of the alternative pathway is found to be more favorable (**T-S$_{bk2}$** stands 6,5 kcal/mol below the reference). The last step is the point of highest energy (**T-S$_{in2}$** is 28,6 kcal/mol above the reference). Now, the **T-S$_{hy}$−S** stands 12.2 kcal/mol above the reference carboxylation state. The free energy goes down to 5.1 kcal/mol for the bond breaking **T-S$_{bk1}$−S** (or −37.3 kcal/mol for **T-S$_{bk2}$−S**) and then raises to 22.7 kcal/mol for the **T-S$_{in1}$−S** (or 36.4 kcal/mol for **T-S$_{in2}$−S**).

TABLE 2: Relative Energies (electronic plus thermal corrections, Δ*E*, kcal/mol), Relative Entropies (Δ*S*, cal/mol K), and Relative Gibbs Free Energies (Δ*G*, kcal/mol) to the Reference T-Ss, Calculated at the Standard Temperature and Pressure of 298.15 K and 1 Atm, Respectively[a]

	Δ*E*	Δ*S*	Δ*G*
	HF/3-21G		
T-S$_{hy}$	−8.67	−39.84	3.21
T-S$_{bk1}$	6.67	−39.99	18.59
T-S$_{in1}$	13.74	−35.85	24.43
T-S$_{bk2}$	−18.67	−40.68	−6.55
T-S$_{in2}$	19.05	−32.14	28.63
T-S$_{hy}$−S	−1.04	−44.37	12.19
T-S$_{bk1}$−S	−12.50	−59.14	5.13
T-S$_{in1}$−S	7.80	−49.94	22.69
T-S$_{bk2}$−S	−51.83	−48.67	−37.32
T-S$_{in2}$−S	19.9	−55.20	36.36
	HF/6-31G**		
T-S$_{hy}$	7.97	−34.22	18.17
T-S$_{bk1}$	18.97	−32.09	28.54
T-S$_{in1}$	22.72	−26.90	30.74
T-S$_{bk2}$	−1.67	−35.87	9.02
T-S$_{in2}$	25.68	−23.63	32.73
T-S$_{hy}$−S	18.95	−39.49	30.72
T-S$_{bk1}$−S			
T-S$_{in1}$−S	21.12	−30.23	30.13
T-S$_{bk2}$−S	−18.66	−41.11	−6.41
T-S$_{in2}$−S	31.88	−42.22	44.47

[a] Total energies and entropies of the references are: **T-S$_{ca}$** plus a water molecule, HF/3-21G, $E = -527.245400$ au, $S = 130.213$ cal/K mol; HF/6-31G**, $E = -530.230759$ au, $S = 125.032$ cal/K mol; **T-S$_{ca}$−S** plus a water molecule, HF/3-21G, $E = -1342.073049$ au, $S = 201.013$ cal/K mol; HF/6-31G**, $E = -1349.606670$ au, $S = 193.496$ cal/K mol.

For comparison we report some values obtained with the 6-31G** basis set. The hydration transition-state has again a barrier that is increased by the presence of magnesium sphere. The bond-breaking step via **T-S$_{bk2}$−S** is again the more favorable. Bond breaking via **T-S$_{bk1}$−S** cannot be fully compared. The reason is that the coordination sphere tends to rearrange itself thereby perturbing the saddle-point character, as commented above. In a more complete model, the coordination sphere displacements will be modulated by interactions with the surrounding protein. Finally, electronic correlation effects

are essential to get a correct description of the bond breaking/forming events found in the transition structures. Small molecular models have to be used with caution. We believe that both the geometry and transition vector are two good indices that gauge the possible mechanistic issues thereby leading energy as a less relevant issue in the present context.

The present theoretical study indicates that the chemistry of Rubisco can be viewed as mediated by a set of intramolecular hydrogen arrangements, with the absence of direct acid−base catalysis by active site side chains; these residues support substrate binding and productive molding which are fundamental for catalysis.

Acknowledgment. This work was supported by research funds of the DGI (Project BQU2000-1425-C03-02). Calculations were performed on two Silicon Graphics Indigo 2 R10000 workstation of the Departament de Ciències Experimentals and on two Silicon Graphics Power Challenger L of the Servei d'Informàtica of the Universitat Jaume I. We are indebted to these centers for providing us with computer capabilities. M.O. thanks the Ministerio de Educación y Ciencia and Jaume I University for FPI fellowships. O.T. is "Profesor Visitante IBERDROLA de Ciencia y Tecnología". We thank IBERDROLA for financial support. O.T. thanks NFR (Sweden) for financial support.

References and Notes

(1) Oliva, M.; Safont, V. S.; Andrés, J.; Tapia, O. *J. Phys. Chem. A* **2001**, *105*, 4726.

(2) Safont, V. S.; Oliva, M.; Andrés, J.; Tapia, O. *Chem. Phys. Lett.* **1997**, *278*, 291.

(3) Oliva, M.; Safont, V. S.; Andrés, J.; Tapia, O. *J. Phys. Chem. A* **1999**, *103*, 8725.

(4) Oliva, M.; Safont, V. S.; Andrés, J.; Tapia, O. *Chem. Phys. Lett.* **1998**, *294*, 87.

(5) Andrés, J.; Oliva, M.; Safont, V. S.; Moliner, V.; Tapia, O. *Theor. Chem. Acc.* **1999**, *101*, 234.

(6) Zhan, C.-G.; Niu, S.; Ornstein, R. L. *J. Chem. Soc., Perkin Trans. 2* **2001**, 23.

(7) Turro, N. J.; Buchachenko, A. L.; Tarasov, V. F. *Acc. Chem. Res.* **1995**, *28*, 69.

(8) Tapia, O.; Andrés, J.; Safont, V. S. *J. Phys. Chem.* **1996**, *100*, 8543.

(9) Moliner, V.; Andrés, J.; Oliva, M.; Safont, V. S.; Tapia, O. *Theor. Chem. Acc.* **1999**, *101*, 228.

(10) Oliva, M.; Safont, V. S.; Andrés, J.; Tapia, O. *J. Phys. Chem. A* **1999**, *103*, 6009.

(11) Tapia, O.; Oliva, M.; Safont, V. S.; Andrés, J. *Chem. Phys. Lett.* **2000**, *323*, 29.

(12) Frisch, M. J.; Trucks, G. W.; Schlegel, H. B.; Gill, P. M. W.; Johnson, B. G.; Robb, M. A.; Cheeseman, J. R.; Keith, T.; Petersson, G. A.; Montgomery, J. A.; Raghavachari, K.; Al-Laham, M. A.; Zakrzewski, V. G.; Ortiz, J. V.; Foresman, J. B.; Cioslowski, J.; Stefanov, B. B.; Nanayakkara, A.; Challacombe, M.; Peng, C. Y.; Ayala, P. Y.; Chen, W.; Wong, M. W.; Andres, J. L.; Replogle, E. S.; Gomperts, R.; Martin, R. L.; Fox, D. J.; Binkley, J. S.; Defrees, D. J.; Baker, J.; Stewart, J. P.; Head-Gordon, M.; Gonzalez, C.; Pople, J. A. *Gaussian 94*; Gaussian, Inc.: Pittsburgh, PA, 1995.

(13) Frisch, M. J.; Trucks, G. W.; Schlegel, H. B.; Scuseria, G. E.; Robb, M. A.; Cheeseman, J. R.; Zakrzewski, V. G.; Montgomery, J. A., Jr.; Stratmann, R. E.; Burant, J. C.; Dapprich, S.; Millam, J. M.; Daniels, A. D.; Kudin, K. N.; Strain, M. C.; Farkas, O.; Tomasi, J.; Barone, V.; Cossi, M.; Cammi, R.; Mennucci, B.; Pomelli, C.; Adamo, C.; Clifford, S.; Ochterski, J.; Petersson, G. A.; Ayala, P. Y.; Cui, Q.; Morokuma, K.; Malick, D. K.; Rabuck, A. D.; Raghavachari, K.; Foresman, J. B.; Cioslowski, J.; Ortiz, J. V.; Baboul, A. G.; Stefanov, B. B.; Liu, G.; Liashenko, A.; Piskorz, P.; Komaromi, I.; Gomperts, R.; Martin, R. L.; Fox, D. J.; Keith, T.; Al-Laham, M. A.; Peng, C. Y.; Nanayakkara, A.; Gonzalez, C.; Challacombe, M.; Gill, P. M. W.; Johnson, B.; Chen, W.; Wong, M. W.; Andres, J. L.; Gonzalez, C.; Head-Gordon, M.; Replogle, E. S.; Pople, J. A. *Gaussian 98*; Gaussian, Inc.: Pittsburgh, P. A., 1998.

(14) *GaussView*, version 1.0; Gaussian, Inc: Pittsburgh, PA 15106, 1997.

(15) Safont, V. S.; Oliva, M.; Andrés, J.; Tapia, O. *Chem. Phys. Lett.* **2000**, *318*, 361.

(16) Oliva, M.; Safont, V. S.; Andrés, J.; Tapia, O. *Chem. Phys. Lett.* **2001**, *340*, 391.

(17) Miziorko, H. M.; Lorimer, G. H. *Annu. Rev. Biochem.* **1983**, *52*, 507.

(18) Lorimer, G. H.; Gutteridge, S.; Reddy, G. S. *J. Biol. Chem.* **1989**, *264*, 9873.

(19) Saver, B. G.; Knowles, J. R. *Biochemistry* **1982**, *21*, 5398.

(20) Lorimer, G. H. *Annu. Rev. Plant. Physiol.* **1981**, *32*, 349.

(21) Schneider, G.; Lindqvist, Y.; Brändén, C.-I. *Annu. Rev. Biophys. Biomol. Struct.* **1992**, *21*, 119.

(22) Andrews, T. J.; Lorimer, G. H. In *The Biochemistry of Plants*; Hatch, M. D., Ed.; Academic Press: Orlando, FL, 1987; Vol. 10.

(23) Cleland, W. W. *Biochemistry* **1990**, *29*, 3194.

(24) Taylor, T. C.; Andersson, I. *J. Mol. Biol.* **1997**, *265*, 432.

(25) Cleland, W. W.; Andrews, T. J.; Gutteridge, S.; Hartman, F. C.; Lorimer, G. H. *Chem. Rev.* **1998**, *98*, 549.

(26) Andersson, I. *J. Mol. Biol.* **1996**, *259*, 160.

(27) Fukui, K. *J. Phys. Chem.* **1970**, *74*, 4161.

(28) Müllhofer, G.; Rose, I. *J. Biol. Chem.* **1965**, *240*, 1341.

(29) Fiedler, F.; Mullhofer, G.; Trebst, A.; Rose, I. A. *Eur. J. Biochem.* **1967**, *1*, 395.

(30) Sue, J. M.; Knowles, J. R. *Biochemistry* **1982**, *21*, 5404.

(31) Van Dyk, D. E.; Schloss, J. *Biochemistry* **1986**, *25*, 5145.

(32) Chène, P.; Day, A. G.; Fersht, A. R. *J. Mol. Biol.* **1992**, *225*, 891.